Measuring intracellular motion using dynamic light scattering with optical coherence tomography in a mouse tumor model

Golnaz Farhat[a,b], Adrian Mariampillai[c,d], Kenneth K. C. Lee[c,e], Victor X. D. Yang[b,c], Gregory J. Czarnota[a,b,f,g] and Michael C. Kolios[a,h]

[a]Medical Biophysics, Univ. of Toronto, Canada;
[b]Imaging Research, Sunnybrook Health Sciences Centre, Toronto, Canada;
[c]Electrical & Computer Engineering, Ryerson University, Toronto, Canada;
[d]Ontario Cancer Institute, University Health Network, Toronto, Canada;
[e]Electrical & Computer Engineering and the Institute for Optical Sciences, Univ. of Toronto, Canada
[f]Radiation Oncology, Sunnybrook Health Sciences Centre, Toronto, Canada;
[g]Radiation Oncology, Univ. of Toronto, Toronto, Canada
[h]Physics, Ryerson University, Toronto, Canada;

ABSTRACT

We present, for the first time an *in vivo* implementation of dynamic light scattering (DLS) adapted to optical coherence tomography (OCT). Human bladder carcinoma tumors were grown in dorsal skin-fold window chambers fitted to male nude mice and imaged at a rate of 200 Hz using OCT. Maps of speckle decorrelation times (DT) were generated for regions of skin from individual mice as well as for regions containing tumor tissue before and after treatment with chemotherapy. Variations in DT were found between individual mice exhibiting different skin anatomy (primarily due to deterioration from the window chamber implantation). A significant difference in DT was also observed between tumor regions and surrounding normal tissue. Finally, maps of DT generated for tumor tissue treated with chemotherapy indicated a drop in DT at 24 and 48 hours after treatment. These preliminary results suggest the feasibility of using DLS-OCT to measure intracellular motion as an endogenous contrast mechanism *in vivo*.

Keywords: cell death, apoptosis, dynamic light scattering, optical coherence tomography, speckle decorrelation, window chamber model, treatment monitoring.

1. INTRODUCTION

In optical coherence tomography (OCT) imaging speckle intensity is dependent on the size, spatial distribution, density and optical properties of scatterers within the resolution volume of the imaging system [1]. In the case of living tissue, the motion of scatterers caused by the flow of red blood cells within the vascular network [2] or intracellular motion within the tissue [3] will induce dynamic changes in the speckle pattern. Examples of intracellular motion include, but are not limited to, the active motion of organelles along microtubules, the passive diffusion of macromolecules and vesicles through the cytoplasm and the reorganization of the cytoskeleton and cytoplasm during mitosis and apoptosis. We hypothesize that the rate of intracellular motion is related to the viability and metabolic state of cells and that it can be used as an endogenous contrast mechanism to detect cell death in the context of cancer treatment monitoring. Intracellular motion can be measured indirectly by detecting variations in speckle intensity in consecutively acquired OCT images. We have previously used speckle variance measurements to detect blood flow and changes in the vascular network of tumors before and after treatment with photodynamic therapy in mice [2]. In order to measure subtle differences in intracellular motion related to cell viability we have adapted a dynamic light scattering (DLS) technique to OCT.

Dynamic light scattering techniques are based on measuring time-dependent fluctuations in scattered light intensity from a sample and relating these fluctuations to physical properties of that sample. This technique has been used extensively in industrial and chemical applications to determine the size distribution, molecular weights and the rotational motion of

Biomedical Applications of Light Scattering VI, edited by Adam P. Wax, Vadim Backman, Proc. of SPIE
Vol. 8230, 823002 · © 2012 SPIE · CCC code: 1605-7422/12/$18 · doi: 10.1117/12.908536

particles in suspension [4]. Examples of the use of DLS for biological applications include the characterization of bacterial growth, the measurement of human sperm motility and the determination of blood flow velocities [5-8]. More recently, DLS has been applied to coherence-domain imaging by using holographic tissue dynamics spectroscopy to measure the response of multicellular tumor spheroids to environmental perturbations such as changes in temperature, osmolarity, pH and growth factors [9].

The work described in this paper uses dynamic light scattering adapted to OCT (DLS-OCT) to detect variations in intracellular motion in a mouse tumor model. We have previously used DLS-OCT *in vitro* to measure changes in intracellular motion cause by apoptosis in acute myeloid leukemia cells treated with cisplatin [10] and in multicellular tumor spheroids to differentiate between the viable rim and necrotic core [11]. The current work is a feasibility study which expands this technique to an *in vivo* model and demonstrates the potential to use DLS-OCT for monitoring cell death during cancer therapy. Human bladder carcinoma cells were inoculated into dorsal skin-fold window chambers implanted into male nude mice. Mice were treated intravenously with cisplatin, a chemotherapeutic known to cause apoptosis [12], and imaged both pre-treatment and at 24 and 48 hours after treatment. The results obtained from this study demonstrate the potential to use DLS-OCT to measure intracellular motion *in vivo*, in particular for assessing cell viability during cancer treatment monitoring.

2. METHODS

2.1 OCT system

A swept source OCT system was used for all *in vivo* studies. The laser design has been previously described in [13]. Briefly, the laser has a center wavelength of 1310 nm and a bandwidth of approximately 110nm with a scan rate of 36kHz. A data acquisition card (ATS460, AlazarTech) was used to acquire raw OCT signal continuously, which was transferred to the memory on a video graphics card (GeForce 9800 GT, NVIDIA). Custom-written kernels together with built-in CUDA libraries (i.e. cudpp, cufft) were used to manipulate and reconstruct OCT images on the multiple cores (112) of the GPU, which enables massive parallel data processing. This allows to dramatically enhance the data throughput when compared to processing using only the CPU, but also concurrently frees up CPU resources. Another advantage for processing data directly on the graphics card is that the reconstructed OCT image can be displayed without any additional memory transactions. The above setup allows real-time acquisition, processing, and display only limited by the A-scan rate of the laser.

2.2 *In vivo* tumor model

The *in vivo* tumor model used in this study consisted of human bladder carcinoma tumors grown within a mouse dorsal skin-fold window chamber model (WCM). Male athymic nude mice (NCRNU-M, Taconic) were implanted with a dorsal skinfold window chamber and a total volume of 10 μl of HT-1376 (ATCC) cells suspended in growth medium was injected into the skin flap at a concentration of 1.5×10^7 cells/mL. Tumors reached 2-3 mm in diameter after approximately 3 weeks. All mice were treated with a tail vein injection of the chemotherapeutic drug cisplatin (100 mg/m^2) on the first day of imaging. Data were acquired immediately prior to cisplatin injection and 24 and 48 hours after. All procedures including surgeries, chemotherapy and imaging were conducted under ketamine-xylazine aneasthesia administered intraperitoneally and with institutional approval at the Princess Margaret Hospital (Toronto, Canada). A total of three animals were used for this pilot study.

2.3 Data acquisition and analysis

For each imaging time point, two-dimensional frames of OCT data were acquired continuously at 200 frames per second over approximately 8 seconds. Each frame contained 180 A-scans and covered a lateral distance of 3 mm. Data sets were acquired from 15 to 25 planes within the window chamber of each mouse. The imaging planes were spaced approximately 200 μm apart and covered both tumor regions and skin-only regions.

Decorrelation maps were generated by calculating decorrelation times (DT) for each pixel location within an imaging plane of data. Each DT was determined by calculating the autocorrelation function of the fluctuating signal and extracting the line width at 1/e of the maximum autocorrelation value. We assume tissue to be a non-ergodic medium which requires removal of the static scattering component from the fluctuating signal in order to determine the correct autocorrelation function. For this study, the static component was determined for a given pixel using a 7 pixel by 7 pixel

region centered at that pixel and following the method described previously in [10]. Spatial averaging of the DT values using a 3 x 3 kernel was used to generate the final decorrelation maps.

2.4 Histological validation

After each imaging time point a single mouse was sacrificed and the dorsal skin contained within the window chamber was excised and fixed in 10% buffered formalin for 48 hours. Subsequently, the tissue was processed for haematoxylin and eosin (H & E) and terminal deoxynucleotidyl transferase dUTP nick end labeling (TUNEL) staining. Microscopy was carried out using a Leica DC 200 digital imaging system (Leica Microsystems GmbH, Germany).

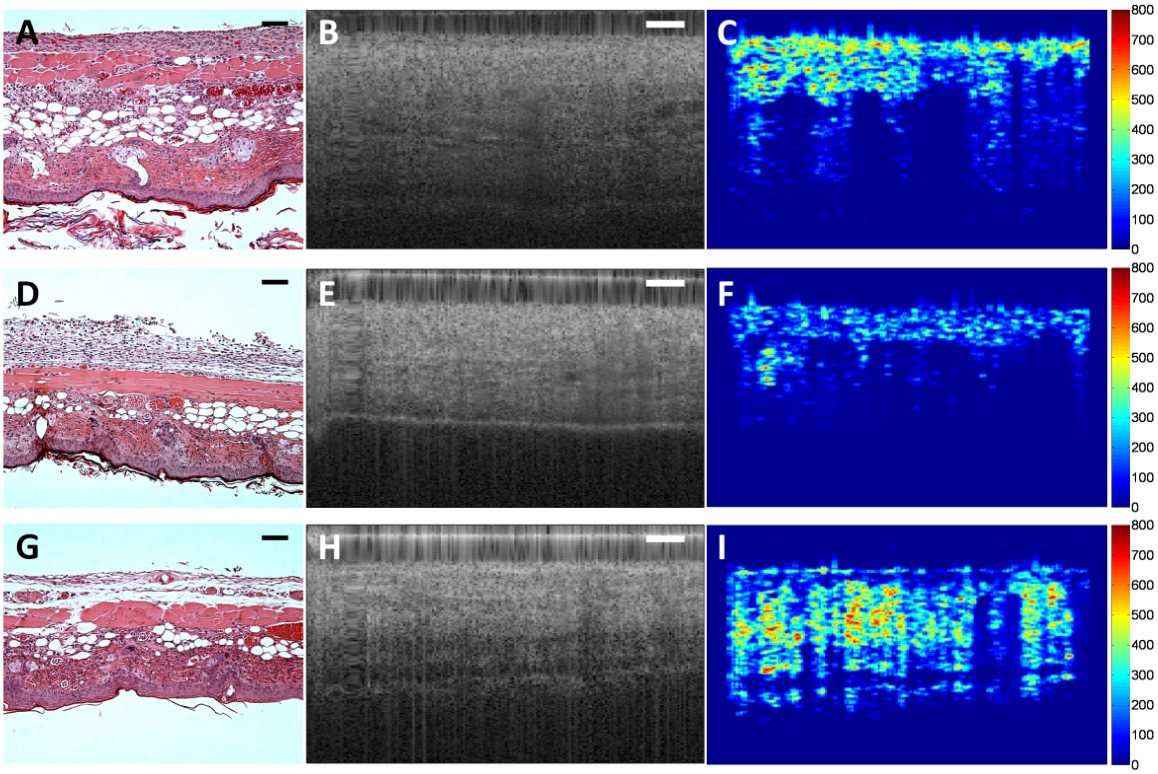

Figure 1. Variations in skin structure. H & E stained sections from the skin of three individual mice (left column). The glass cover slip of the window chamber was positioned at the top of each of the images in this panel, with the epidermal layer located at the bottom. Corresponding B-mode images (middle column) and maps of decorrelation time (right column) acquired using OCT. Scale bars in the histology and OCT images indicate 50 μm and 300 μm, respectively. Decorrelation times in ms are indicated by color bars on the right.

3. RESULTS AND DISCUSSION

3.1 Inter-mouse variations in skin structure

Histological sections of skin tissue stained with H & E revealed significant differences in the skin's layered structure between the three mice. Since the animals lived with the dorsal skinfold window chambers for a period of three weeks, it is not surprising to detect signs of skin deterioration in some of the animals. Figure 1 displays sections of skin obtained from three individual mice in the left column. These images demonstrate variations in overall skin thickness, the thickness of the different layers within the skin, as well as the structure of these layers. B-mode OCT images acquired from approximately the same regions are shown in the middle column of figure 1. The differences in overall skin thickness correspond well to what was observed in the H & E sections. The distinct layers contained within the skin are easily observed in figure 1B where the layers are best preserved. Variations in the OCT image intensity of these layers

are also observed between the three mice. In figure 1E the various skin layers are more difficult to observe, presumably because of the deterioration of the skin as seen in figure 1D. The decorrelation maps in figure 1 (right column) indicate distinct patterns of intracellular motion observed between the skin of the three mice. Again we see the largest differences between various layers observed in the top and bottom rows while a lack of layered structure is seen in the middle row. Given the small number of animals in this study, it would be premature to explain these variations; however, these results help to demonstrate the feasibility of measuring intracellular motion *in-vivo*.

3.2 Speckle decorrelation in skin versus tumor regions

An OCT b-mode image (figure 2A) consisting of a cross section through the centre of a tumor indicates a drop in backscatter intensity within the tumor as compared to the surrounding skin. A decorrelation map (figure 2B) generated from the same cross-section indicates a significant difference in speckle DT between the two types of tissue. The DT from a region within the tumor is 50 to 200 ms while the surrounding skin decorrelates more slowly with DTs ranging between 150 to 500 ms. Average autocorrelation functions (figure 2C) generated from areas within the skin and tumor regions further demonstrate the difference in the DT between the two tissue types. We suspect that the shorter DTs within the tumor are due to higher metabolic activity of tumor cells compared to cells from the surrounding skin. An additional interesting feature of this data includes the presence of blood vessels indicated by regions of very low (near zero) DT.

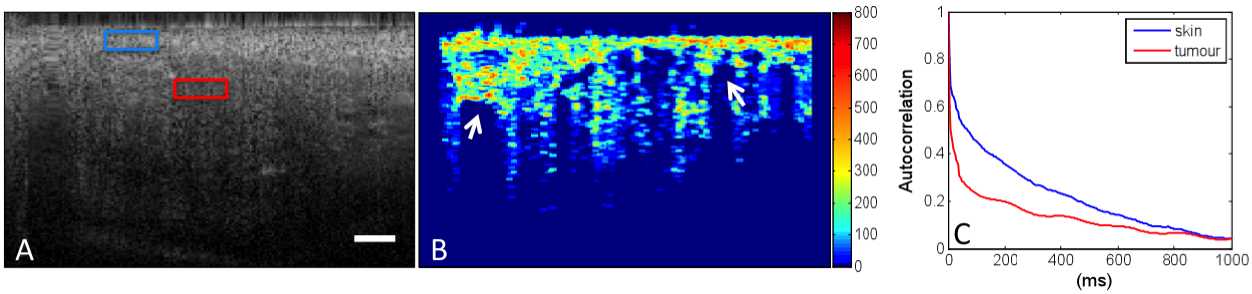

Figure 2. Comparing decorrelation in skin versus tumor tissue. B-mode OCT image (A), decorrelation map (B) and average autocorrelation functions obtained from regions of skin and tumor highlighted in A (C). White arrows point to regions of blood flow represented by very low DT. Scale bar in the OCT image is 300 μm and the decorrelation times in ms are indicated by the color bar.

3.3 Treatment monitoring

Optical coherence tomography images (figure 3) acquired from a tumor at 0 hours, 24 hours and 48 hours after injection with cisplatin indicate a progressive increase in backscatter intensity (figure 3 A, C, E). This change parallels the variations in cellular structure and density observed in H & E stained histological sections. As shown in figure 4 (A and B), we observe a decrease in cell number density in the tumor 48 hours after the cisplatin treatment. Additionally, the cells in the untreated tumor display clearly defined nuclei with a punctate chromatin pattern. The cells in the treated tumor are lacking this feature and the nuclei are less clearly defined - while in the same image a number of cells are lacking a visible nucleus altogether. TUNEL stained sections (figure 4, B and D) reveal dark brown staining of the cells in the treated tumor (compared to untreated), which is indicative of apoptosis. A similar trend in backscatter intensity was observed in a previous *in vitro* study where acute myeloid leukemia cell samples were treated with cisplatin to induce apoptosis [14].

Decorrelation maps overlayed onto B-mode structural images in figure 3 indicate an increase in DT from 0 to 48 hours. The colorbar in the figure indicates a more narrow range of DT that is representative of the tumor values compared to the values measured in the skim. The increase in DT as a function of time after treatment indicates a potential reduction in intracellular motion. This may be due to a reduction in the number density of cells and / or to a loss of cell viability in the tumor tissue. These results correspond to data acquired from a single mouse, therefore, further study is required to determine whether the observed changes are reproducible. However, this is the first time such changes in DT have been

observed *in vivo*, indicating the potential to use intracellular motion as an endogenous contrast mechanism for assessing cell viability in the context of cancer treatment monitoring.

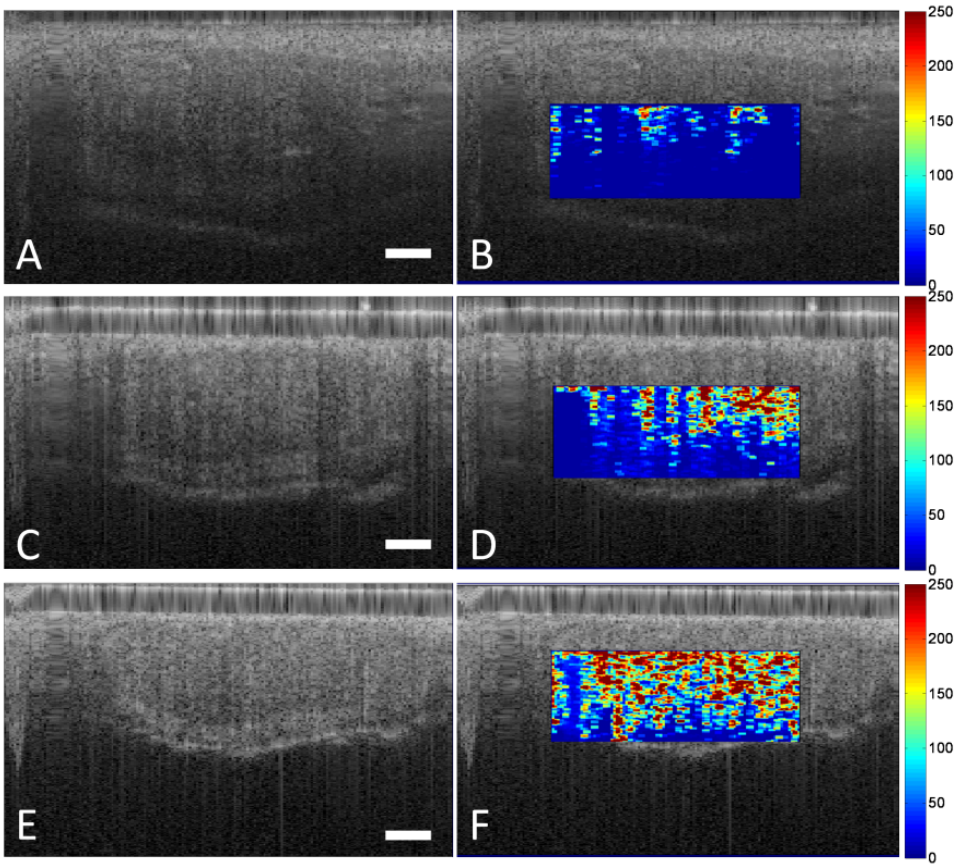

Figure 3. OCT B-mode images (left column) and corresponding overlay of decorrelation time (right column). All images are obtained from the same animal, with the untreated tumor shown in (A, B), the tumor 24 hours after cisplatin treatment in (C, D) and 48 hours after cisplatin treatment in (E, F). Scale bars indicate 300 μm and decorrelation times in ms are indicated by the color bars.

4. CONCLUSIONS

In summary, we have implemented, for the first time, a dynamic light scattering technique using OCT to measure intracellular motion *in vivo*. Decorrelation maps generated for skin measurements within a mouse dorsal skinfold window chamber indicated variations in the patterns of DT between three individual mice for which histological sections demonstrated structural differences in the skin's layered structure. A comparison of DT between skin and tumor tissue indicated a faster decorrelation for regions contained within the tumor, potentially due to higher metabolic activity of tumor cells. Finally, decorrelation maps generated for tumor data acquired before and after cisplatin treatment indicated an increase in DT in the tumor tissue over a 48-hour period. This may be caused by a loss of cell viability and a reduction in cell density within the treated tissue. Given the limited number of animals (n=3) used in this study, it is not possible to draw definite conclusions from the results presented. The intention of this work was to demonstrate the feasibility of using the OCT-DLS technique for measuring intracellular motion and for assessing cell viability. Future work includes developing a segmentation method based on the DT to separate tissue regions from blood vessels. Furthermore, we are currently conducting a more detailed study using a larger number of animals to demonstrate the repeatability of this method as well as to further explore the possibility of using it as a reliable method of treatment monitoring *in vivo*.

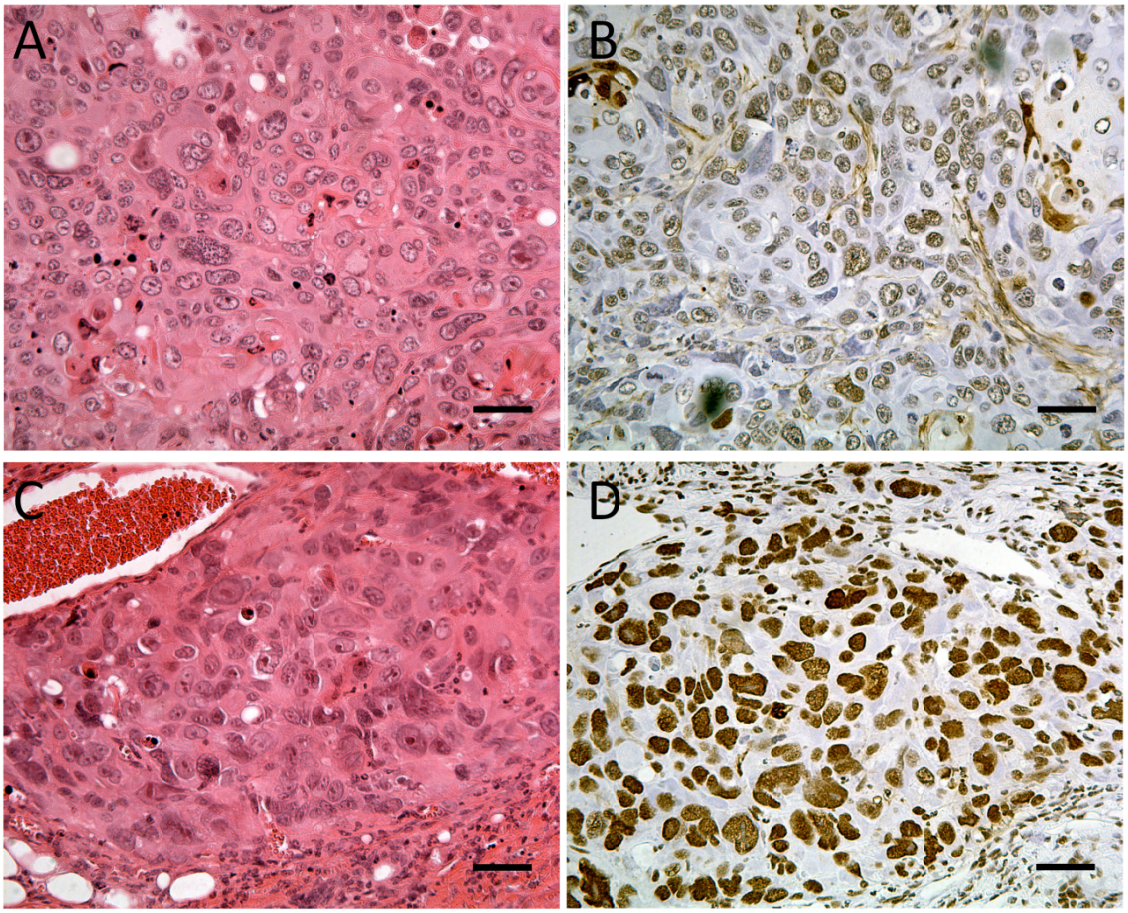

Figure 4. Histological sections obtained from tumors. H & E stained sections (left column) and TUNEL stained sections (right column) of tumor tissue prior to (top row) and 48 hours after cisplatin treatment (bottom row). Scale bars indicate 30 μm.

5. ACKNOWLEDGMENTS

The authors would like to acknowledge Dr. Brian Wilson for kindly providing the facilities and support for animal work conducted at the Ontario Cancer Institute in the Princess Margaret Hospital (Toronto, Canada) and Dr. Alex Vitkin for useful scientific discussions. We would also like to thank Emily Chen for performing the animal surgeries, Azusa Maeda for assisting with tail vein injections as well as Dr. Azza Al-Mahrouki and Anoja Giles for their technical support.

6. REFERENCES

[1] Schmitt, J., Xiang, S. and Yung, K., "Speckle in optical coherence tomography," Journal of Biomedical Optics, 4, 95 (1999).

[2] Mariampillai, A., Standish, B. A., Moriyama, E. H., Khurana, M., Munce, N. R., Leung, M. K., Jiang, J., Cable, A., Wilson, B. C., Vitkin, I. A. and Yang, V. X., "Speckle variance detection of microvasculature using swept-source optical coherence tomography," Opt Lett, 33(13), 1530-2 (2008).

[3] Jeong, K., Turek, J. and Nolte, D., "Volumetric motility-contrast imaging of tissue response to cytoskeletal anti-cancer drugs," Optics Express, 15(21), 14057-14064 (2007).
[4] Berne, B. and Pecora, R., [Dynamic Light Scattering] Dover Publications Inc., New York(1976).
[5] Miike, H., Hideshima, M., Hashimoto, H. and Ebina, Y., "Dynamic Laser-Light Scattering Study on Bacterial Growth," Japanese Journal of Applied Physics, 23(8), 1129-1132 (1984).
[6] Berge, P., Volochine, B., Billard, R. and Hamelin, A., "[Demonstration of the characteristic movement of living microorganisms owing to the study of the inelastic diffusion of light]," C R Acad Sci Hebd Seances Acad Sci D, 265(12), 889-92 (1967).
[7] Tanaka, T. and Benedek, G. B., "Measurement of the Velocity of Blood Flow (in vivo) Using a Fiber Optic Catheter and Optical Mixing Spectroscopy," Appl Opt, 14(1), 189-96 (1975).
[8] Boas, D. A. and Yodh, A. G., "Spatially varying dynamical properties of turbid media probed with diffusing temporal light correlation," Journal of the Optical Society of America A, 14(1), 192-215 (1997).
[9] Nolte, D. An, R. Turek, J and Jeong, K., "Holography tissue dynamics spectroscopy," Journal of Biomedical Optics, 16(8), 087004 (2011).
[10] Farhat, G., Mariampillai, A., Yang, V. X. D., Czarnota, G. J., Kolios, M. C., "Detecting apoptosis using dynamic light scattering with optical coherence tomography," Journal of Biomedical Optics, 16(7), 070505 (2011).
[11] Farhat, G., Mariampillai, A., Yang, V. X. D., Czarnota, G. J., Kolios, M. C., "Optical coherence tomography speckle decorrelation for detecting cell death," Proc. of SPIE Vol. 7907 790710-1:10 (2011).
[12] Zamble, D. and Lippard, S., "Cisplatin and DNA repair in cancer chemotherapy," Trends in biochemical sciences, 20(10), 435-439 (1995).
[13] Yun, S.H. , Boudoux, C., Tearney, G.J., Bouma, B. E., "High-speed wavelength-swept semiconductor laser with polygon-scanner-based wavelength filter," Optics Letters, 28, 2321-2323 (2003).
[14] Farhat, G., Yang, V. X. D., Kolios, M. C., Czarnota, G. J., "Cell death monitoring using quantitative optical coherence tomography methods", Proc. of SPIE, 7907, 790713-1:9 (2011).